Available online at www.sciencedirect.com
ScienceDirect
International Journal of Pharmaceutics 349 (2008) 274–282
INTERNATIONAL JOURNAL OF PHARMACEUTICS
www.elsevier.com/locate/ijpharm

Pharmaceutical Nanotechnology

Preparation and characterization of sodium ferulate entrapped bovine serum albumin nanoparticles for liver targeting

Feng-Qian Li [a,*], Hua Su [a,b], Jing Wang [a], Ji-Yong Liu [a], Quan-Gang Zhu [a], Yi-Bo Fei [a], Yong-Hua Pan [a], Jin-Hong Hu [a,*]

[a] *Department of Pharmaceutical Sciences, Changhai Hospital, Second Military Medical University, Shanghai 200433, China*
[b] *Pharmaceutical Division, General Hospial of Nanjing Military Region, Nanjing 210002, China*

Received 8 October 2006; received in revised form 28 May 2007; accepted 8 August 2007
Available online 11 August 2007

Abstract

Sodium ferulate (SF) loaded nanoparticles were prepared by desolvation procedure and subsequent cross-linking of the wall material of bovine serum albumin (BSA). Several factors in the nanoencapsulation process, such as the addition rate of the desolvation agent, composition of BSA and SF solution, amount of the cross-linker glutaraldehyde, were investigated to elucidate their influences on the particle size, zeta potential, drug loading and encapsulation efficiency of the resulted nanoparticles. The obtained spherical nanoparticles were negative charged with zeta potential from −20 to −40 mV, and characterized between 100 and 200 nm with a narrow size distribution. In the condition of introducing 1.0 mL 8% glutareldehyde per mg of BSA, the drug entrapment efficiency (EE) of 80% (w/w) and loading capacity of about 16% (w/w) could be achieved for the cross-linked BSA nanoparticles with SF encapsulated (SF-BSA-NP). And the drug EE was decreased along with the increasing amount of glutareldehyde used for cross-linking. The *in vitro* drug release properties of SF-BSA-NP behaved with an initial burst effect and then sustained-release stage. To some extent, the drug release rate could be adjusted by cross-linking with different amount of glutaraldehyde. Compared with SF solution, SF-BSA-NP showed a much higher drug distribution into liver and a lower drug concentration in other tissues, after intravenously injected to mice. So, BSA based nanoparticles might be a suitable controlled released carrier for the freely water-soluble drug SF and further hepatic targeted drug delivery.

Keywords: Sodium ferulate; Bovine serum albumin; Nanoparticles; Desolvation; Liver-targeted delivery

1. Introduction

With the achievements of available pathologic and serologic markers for ongoing fibrogenesis, experimental and clinical anti-fibrotic trials have become more active. However, therapeutic attempts with anti-fibrotic drugs are still at an experimental stage. Some potential agents for hepatic fibrosis, such as colchicine, gamma-interferon, inhibitors of prolyl hydroxylase, and malotilate, must be further evaluated in controlled clinical trials (Wu and Danielsson, 1994). In addition, almost all anti-fibrotic agents are neither liver nor fibrosis specific. Some site-directed carriers like liposomes and nanoparticles, used as vesicles for hepatic targeted drug delivery, might improve efficacies and reduce adverse effects of the anti-fibrotic ingredients (Yao et al., 1995; Li and Hu, 2002).

Sodium ferulate (SF) or 3-methoxy-4-hydroxy-cinamate sodium has been used for cardiovascular and cerebrovascular diseases clinically in China (Wang and Ou-Yang, 2005). Recent studies had illuminated the potential anti-hepatic fibrosis effect of SF (Wang et al., 1997; Liu et al., 2000). The involved antioxidation mechanism might be due to its phenolic nucleus and unsaturated side chain, readily to form resonance-stabilized phenoxy radicals (Castelluccio et al., 1996). *N*-Dodecyl-ferulate, a novel potential sunscreen, had been incorporated into lipid matrix to form aqueous solid lipid nanoparticles dispersions with the high pressure homogenization technique (Souto et al., 2005). Synthesized SF was frequently used as the active agent to prepare several commercialized dosage forms of SF injections, oral tablets or powders. Then, the further development of

* Corresponding authors. Tel.: +86 21 25070674; fax: +86 21 25070668.
E-mail addresses: fqlijr@gmail.com (F.-Q. Li), hujh@smmu.edu.cn (J.-H. Hu).

0378-5173/$ – see front matter © 2007 Elsevier B.V. All rights reserved.
doi:10.1016/j.ijpharm.2007.08.001

liver-targeted delivery system of SF would be promising and inspiring for those suffered from hepatic fibrosis.

Mainly delivered to the mononuclear phagocytes system (MPS), the association of a drug to nanoparticles or liposomes could change the drug biodistribution profile. As the liver is the largest reticuloendothelial organ in the body, macrophages in liver (i.e., Kupffer cells) are attractive candidates to serve as the effector cells for therapy of hepatic diseases (Grislain et al., 1983; Yamashita et al., 1991; Daemen et al., 1995; Konno et al., 1997). The body distribution and opsonization of colloidal drug carrier systems by macrophages seem to be influenced by their particle sizes and surface characteristics (Tröster et al., 1990; Harashima et al., 1994; Moghimi et al., 2001; Ishida et al., 2003). Although the carrier systems of nanoparticles or liposomes could not directly reach the hepatocytes, the uptake of intravenously injected particulate drug carriers by MPS cells might as well be the main limiting factor in the efficient targeting of a drug to the Kupffer cells in the liver (Klibanov et al., 1990). A number of attempts have been made to indicate the accumulation of conventional nanoparticles and liposomes (when intravenously injected) into the liver with a significant fraction (Mbela et al., 1992; Zhang et al., 1996; Ogawara et al., 2004; Liang et al., 2006; Kamruzzaman Selim et al., 2007). Among various colloidal drug delivery systems, nanoparticles could permeate through biological barriers after intravenous administration because of their small size (Nakada et al., 1996; Song et al., 1997; Williams et al., 2003). The feasibility of particles ranged in 50–200 nm to arrive at fenestration in the hepatic sinusoidal endothelium, might lead to hepatic accumulation after intravenous injection. As a consequence, a major aspect in preparing a targeted drug carrier lies in the establishing procedure conditions which could control the resulting particle size with a narrow distribution.

Due to the well biocompatibility and biodegradability, serum albumin was most often used as the natural wall material for nanoencapsulation. Generally three different methods about emulsion formation, desolvation or coacervation were applied for albumin nanoparticles preparation. With respect to emulsion technique, removal of the organic residues was needed (Müller et al., 1996). The major shortcoming for coacervation was that the pH value, adjusted in the absence of salt, might be usually limited in reliability (Lin et al., 1993). Desolvation process of albumin with organic solvents followed by cross-linking with glutaraldehyde is commonly used to assemble protein nanoparticles (Marty et al., 1978). Previous studies (Zimmer et al., 1994a,b; Merodio et al., 2001) have described the desolvation of albumin to produce nanoparticles. The alternative method of desolvation procedure was systematically characterized to establish a rational basis for the production of albumin nanoparticles (Weber et al., 2000; Langer et al., 2003).

In this paper, a nanoencapsulation procedure of desolvation and subsequent cross-linkage was used to prepare the SF loaded bovine serum albumin (BSA) nanoparticles (SF-BSA-NP) for liver targeting. A systematic investigation concerning the influence of albumin content, cross-linking agent and the flow rate of desolvation reagent on nanoparticles size and zeta potential was carried out. In addition, the nanoparticle yield, drug entrapment efficiency, release properties *in vitro* and tissue distribution *in vivo* were also tested in the present work.

2. Materials and methods

2.1. Reagents, chemicals and animals

Sodium ferulate was obtained from Limin Pharmaceutical Factory of Lizhu Group (Shaoguan, China). Bovine serum albumin was purchased from Sino-American Biotechnology Company. Ethanol and 25% glutaraldehyde solution (v/v) were obtained from the Chemical Agent Station, Medicine Group of China. BCA albumin concentration measurement kit (Biyuntian biotechnology institute, Haimen, China). HPLC grade methanol and acetic acid came from Sigma–Aldrich Chemie GmbH (Steinheim, Germany). All other chemicals were of analytical grade.

Kunming mice (20 ± 2 g) were supplied by the experimental animal center of Second Military Medical University (Shanghai, China). All procedures described in this study were approved by the Animal Care and Supply Committee of Second Military Medical University.

2.2. Preparation of SF loaded BSA nanoparticles

According to Weber et al. (2000) and Langer et al. (2003), the desolvation technique was applied for the preparation of SF-BSA-NP. SF was dissolved in distilled water together with BSA in different ratio from 2:1 to 16:1 (BSA:SF, w/w). Subsequently, 2 mL desolvation agent of ethanol was added dropwise into the aqueous albumin solution under magnetic stirring (500 rpm). Opalescent suspension was formed spontaneously at room temperature, and was further examined as nanoparticles. Addition of ethanol at a defined rate (0.5–1.0 mL/min) might enable the nanoencapsulation process to be controlled. After the desolvation process, 8% glutaraldehyde in water (v/v) was added to cross-link the desolvated BSA nanoparticle. And the cross-linking process was performed under stirring of the colloidal suspension over a time period of 12 h. The detailed formation conditions were shown in the corresponding legends and figures.

Ethanol in the prepared sample was eliminated by evaporation under reduced pressure. Finally, the resulting nanoparticles were purified and obtained by centrifugation at $20{,}000 \times g$ at 12 °C for 30 min before lyophilization.

2.3. Determination of albumin nanoparticle yield

As for the added BSA, only the desolvated BSA participated in the nanoencapsulation process. After quantification of the nondesolvated BSA, the yield of nanoparticles (Y_{np}) could be calculated as the follow equation:

$$Y_{np} = \frac{W_{total\,BSA} - W_{free\,BSA}}{W_{total\,BSA}} \times 100\%$$

where $W_{total\,BSA}$ is the total amount of BSA and $W_{free\,BSA}$ is the amount of free BSA nondesolvated.

For the determination of the nondesolvated BSA, the nanoparticles were separated from the supernatant by centrifugation at 16,000 × *g* for 20 min at room temperature. An aliquot of the supernatant was diluted with distilled water and the amount of the dissolved BSA in the supernatant was determined using a standard BCA protein assay (Smith et al., 1985).

2.4. Morphology of nanoparticles

A few drops of the diluted nanoparticle suspension were deposited onto a carbon-coated copper grid. After 1–2 min of immobilization, the excess solution was wicked off with filter paper and replaced with sodium phosphotungstate solution (0.2%, w/v) for negative staining. Thirty seconds later, the grids were washed twice with distilled water and allowed to dry. And then the morphological examinations of the prepared albumin nanoparticles were performed by an H-600 transmission electron microscope (TEM) (Hitachi, Japan).

2.5. Determination of particle size and zeta potential

The prepared SF-BSA-NP were thereafter analyzed for their volume based particle size and surface electrical charge by electrophoretic light scattering (ELS) method. The size and charge analysis were completed using a Coulter NicompTM 380 ZLS (Santa Barbara, CA, USA), allowing characterization of the size distribution in distilled water (laser droppler velocimetry) and assessment of zeta potential in 0.01% NaCl (particle electrophoretic mobility). The measurements were performed in triplicate at a temperature of 25 °C and a scattering angle of 90° in 4 mm diameter cells with field strength of 10 V/cm.

Polydispersity index (PI) is usually tested to indicate the particle diameter distribution range. The PI value and particle size of nanoparticles could be measured simultaneously by ELS method at the conditions described above.

2.6. Determination of SF loading capacity and encapsulation efficiency

The drug encapsulation efficiency and loading capacity of SF-BSA-NP prepared with different formulations were determined by centrifugation of the colloidal samples at 20,000 × *g* and 12 °C for 30 min. The amount of SF entrapped within nanoparticles was calculated by the difference between the total amount used and the amount presented in the aqueous supernatant phase. The non-entrapped SF in the supernatant obtained after ultracentrifugation of nanoparticles was determined by HPLC method. Each sample was assayed in triplicate.

The HPLC analyses were carried out using a system (Shimadzu, LC-10A, Japan) consisted of two LC-10AT pumps (Shimadzu), a Rheodyne 7125 manual injection valve with 20 μL sample loop, an SPD-10A UV detector (Shimadzu), and C-18 reversed phase column (4.6 mm × 150 mm, 5 μm, Kromasil, Bohus, Sweden). The mobile phase was a mixture of methanol and 0.5% acetic acid (60:40, v/v). The flow rate was 0.8 mL/min at 25 °C, and the wavelength was set at 320 nm.

The SF loading capacity (LC) of nanoparticles and encapsulation efficiency (EE) of the process were calculated as indicated below:

$$\mathrm{LC} = \frac{W_{\text{total SF}} - W_{\text{free SF}}}{W_{\text{np}}} \times 100\%$$

$$\mathrm{EE} = \frac{W_{\text{total SF}} - W_{\text{free SF}}}{W_{\text{total SF}}} \times 100\%$$

where $W_{\text{total SF}}$ is the total amount of SF, $W_{\text{free SF}}$ the amount of free SF and W_{np} is the nanoparticles weight.

2.7. SF release from the nanoparticles in vitro

The *in vitro* drug release profiles of SF-BSA-NP were determined as follows. About 20 mg nanoparticles were re-dispersed in phosphate-buffered saline (PBS, pH 7.4) and placed in a dialysis membrane bag with a molecular cut-off of 8 kDa. Then the SF-BSA-NP contained bag was tied and put into 100 mL of PBS medium. The entire system was incubated at (37 ± 0.5) °C under stirring at 50 rpm. At designated time intervals, 0.5 mL of the release medium was removed and replaced with the same volume of fresh PBS solution. The amount of SF in the release medium was determined by HPLC at the described chromatographic conditions. All measurements were performed in triplicate.

2.8. Tissue distribution

In order to study the *in vivo* biodistribution of SF loaded nanoparticles, SF-BSA-NP and SF solution were injected intravenously to mice via the lateral tail veins severally. Fifty-four mice were fasted overnight and then divided randomly into two groups received SF-BAS-NP and SF solution at the same dosage (0.8 mg SF/kg body weight) individually. In all experiments the total volume of injection was between 0.4 and 0.6 mL/animal.

The biodistribution of SF in mice was performed respectively at 0.5, 1, 2, 4, 6, 8, 12 and 24 h after administration. At these time intervals, the blood was collected and animals were sacrificed to excise the heart, liver, spleen, lung and kidney. The organs were absorbed dry with filter paper, then weighed and frozen. Homogenates were prepared immediately prior analysis. Quantification of SF for the extracted samples was carried out referring to the established reversed-phase HPLC method (Li et al., 2007).

2.9. Statistical analysis

Data were presented as mean ± S.D. Results of the *in vivo* biodistribution studies were analyzed using Student's *t*-test. Differences were considered to be significant at a level of $p < 0.05$.

3. Results and discussion

3.1. Desolvation method for SF loaded nanoparticle preparation

Results in the literature (Weber et al., 2000) have shown the desolvation method for albumin nanoparticles preparation. Furthermore, a controlled desolvation procedure was optimized to achieve a colloidal system of blank albumin nanoparticles with well-defined physicochemical characteristics (Langer et al., 2003). While addition of ethanol into the protein solution, BSA is phase separated as its diminished water-solubility. Nanoparticles were then formed from the albumin solution with the desolvation function produced by ethanol. The added carrier material of BSA had been formed into nanoparticles considerably, and a particle yield of above 90% could be obtained (measured by the BCA protein assay).

The morphologically formed albumin particles not sufficiently stabilized could consequently redissolve again after dispersed with water and then lack an adjustment in drug release rate (Weber et al., 2000; Li et al., 2001). BSA protein, including 60 amino moieties in lysine residues and 26 arginine moieties in guanidino side chains (Meziani and Sun, 2003), might be solidified by condensation reaction with the aldehyde-group contained reagent. So, cross-linking with glutaraldehyde was necessary for stabilization of the desolvated BSA nanoparticles. And the cross-linking process plays a major role in the stability and drug release of the desolvated BSA nanoparticles (Merodio et al., 2001).

The amount of free amino groups may be considered as a measure for the degree of cross-linkage and attributed to the stability of the protein particles (Rubino et al., 1993). As already reported by Weber et al. (2000) for desolvated human serum albumin particles, the lowest required glutaraldehyde concentration for the production of stable nanoparticles appeared to be about 40%. And a reaction time of 24 h for sufficient cross-linking of all amino groups is imperative. The incubation period should compromise the stability and drug release property of the albumin nanoparticles. In this work, the cross-linking step was attentively performed for a period of 12 h with relatively low amounts of glutaraldehyde. The further obtained results of drug loading and release characteristics for the biodegradable SF-BSA-NP, also elucidated the practical cross-linking condition.

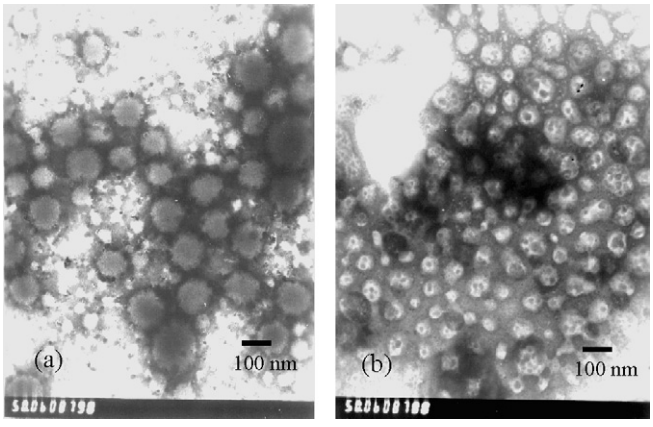

Fig. 1. TEM photograph of blank nanoparticles (a) and drug loaded nanoparticles (b) (50,000×).

Typical TEM image of the nanoparticles and their surface morphology were shown in Fig. 1. As observed from Fig. 1, these nanoparticles appeared spherical in shape with a relatively narrow size distribution. Compared to the blank BSA nanoparticles (Fig. 1A), a similar morphology was also observed for SF-BSA-NP (Fig. 1B) taking spherical shape. Apparently, the entrapped drug was uniformly located within the core-shell like nanoparticles, seemingly immersed in a small pot coated with BSA protein.

3.2. Factors influencing the size and zeta potential of SF-BSA-NP

3.2.1. Ratio of BSA to SF

Fig. 2A shows the influences of BSA/SF ratio on particle diameter and zeta potential of the resulted nanoparticles. It could be seen that the diameters decreased with the rising content of BSA, during the BSA:SF ratios ranged from 2:1 to 8:1 (w/w). In the initial stage of nanoparticle formation, diameter of the sparsely scattered particle was primarily affected by the charges among the colloids suspension. The repelling forces among the negative charged particles enhanced the surface polymerization, while the number of nanoparticles increased. This is somewhat similar to the results of Langer et al. (2003) who had showed a slight influence of the increased albumin concentration on the particle diameter. Probably due to the shielding function of the additional surface charges (even not changed significantly), the following accreted particle size was achieved while the further BSA/SF ratio increased. As a result, the formation of nanoparticles is feasible at BSA:SF ratios between 2:1 and 16:1 (w/w). When the BSA to SF ratio exceeded 16:1, aggregates with large diameter appeared. Continued increasing of BSA ratio made the encapsulation proceed very difficultly.

Based upon the isoelectric point (about 4.4) of BSA, the negative charged nanoparticles were formed in the neutral aqueous medium. Nearly independent of the BSA content, zeta potentials of nanoparticles kept relatively steady around −25 mV without marked diversity (Fig. 2A). And the diameter PI of the prepared SF-BSA-NP showed a tendency to rise while the BSA concentration increased.

3.2.2. Concentration of glutaraldehyde

The desolvated BSA nanoparticles were treated with different amounts of glutaraldehyde to investigate the effect of cross-linking process on their particle size and zeta potential. After desolvation procedure, the formed albumin nanoparticles were cross-linked with 0.54–1.16 μL of 8% glutaraldehyde per mg BSA. These glutaraldehyde contents were necessary for cross-linking the amino moieties in lysine residues of BSA molecules in the particle matrix.

As for the reported studies of desolvated human serum albumin nanoparticles (Weber et al., 2000; Langer et al., 2003), amount of glutaraldehyde used to sufficiently stabilize the albumin nanoparticles was relative to the theoretic amount required for the cross-linkage of all amino groups. Nearly no influence

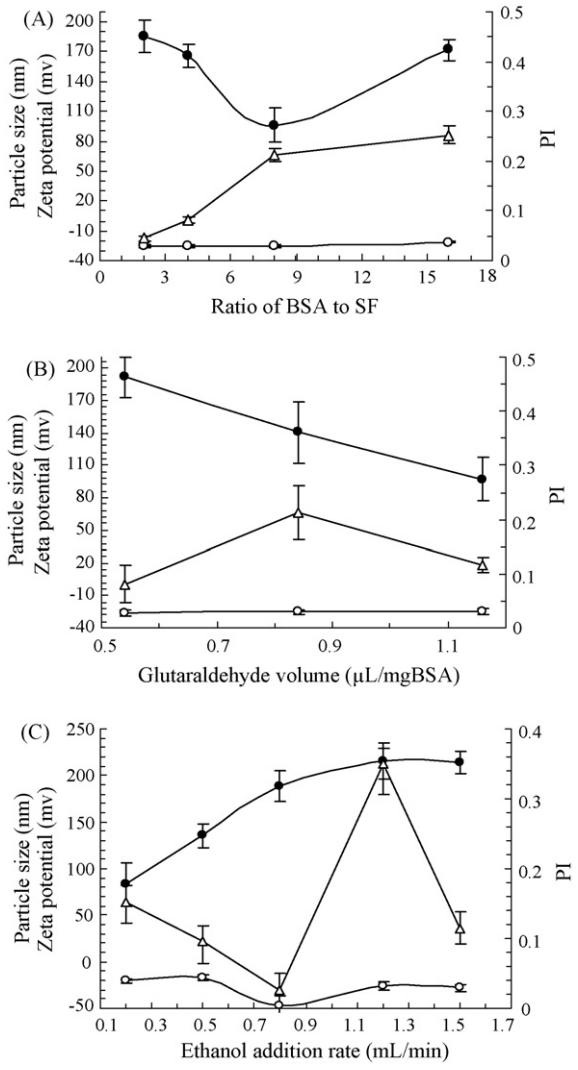

Fig. 2. Particle size (●), zeta potential (◯) and polydispersity index (△) of SF-BSA-NP influenced by the ratio of BSA to SF (A) (ethanol addition rate 0.8 mL/min, amount of SF 12.5 mg, initial BSA concentration 6.25 mg/mL); amounts of 8% glutaraldehyde solution (B) (ethanol addition rate 1.0 mL/min, amount of SF 12.5 mg, rate of BSA to SF 2:1); ethanol addition rate (C) (BSA concentration 12.5 mg/mL, rate of BSA to SF 2:1) (mean ± S.D., $n = 3$).

of the cross-linking conditions on the resulting particle size was observed. In this work, SF entrapped BSA nanoparticles was cross-linked with low amounts of glutaraldehyde for comparable short duration of 12 h. As outlined in Fig. 2B, a remarkable decrease in particle size of SF-BSA-NP might be resulted from the increasing amount of glutaraldehyde used for protein cross-linkage. The mean diameter of nanoparticles decreased from 191.4 nm (0.54 μL cross-linker) to 91.5 nm (1.16 μL cross-linker). The enhanced cross-linking degree could be expected for such reduction in diameter of the close-up constructed nanoparticles with conceivable high bulk density. Whereas the cross-linking degrees could not influence the resulting zeta potential (about −25 mV) and PI (smaller than 0.2) significantly (Fig. 2B).

3.2.3. The rate of ethanol addition

The desolvation process can be divided into two parts; a first part where an increase in desolvation agent leads to an increase in particle size and a second part where the particle size remains constant but the particle concentration is still increasing (Weber et al., 2000). The rate of desolvation was changed accordingly to investigate the resulting particle size. It could be seen from Fig. 2C, the ethanol addition rate (0.2–1.5 mL/min) showed significant influence on the average diameter of the BSA nanoparticles (increased from 83 to 215 nm). Thereby, the puff-structured nanoparticles were formed with relatively large diameter. This might be due to the fast albumin-phase separation rate caused by the added ethanol. The quick desolvation process might as well lead to large aggregates of BSA or precipitation of SF. So the ethanol induced desolvation rate should be controlled in the proper range for drug-aimed nanoencapsulation.

The rate of ethanol addition also mainly influenced the particle size distribution range. As shown in Fig. 2C, a rate smaller than 0.5 mL/min or exceed 0.8 mL/min led to more un-uniformly sized nanoparticles. Accordingly, nanoparticles with a PI less than 0.10 could be obtained at the ethanol addition rate between 0.5 and 0.8 mL/min. The zeta potential of the nanoparticles was reduced to about −48 mV at the ethanol addition rate of 0.8 mL/min. While in other cases, the values of zeta potential were about −25 mV which is in accordance with the earlier results of Lin et al. (1994) and Weber et al. (2000). The decreased zeta potential (to −48 mV) indicated a progressive cross-linking reaction of glutaraldehyde with the positively charged amino groups at the BSA nanoparticle surface. Electric contribution of the negatively charged carboxylic groups became stronger and the zeta potential decreased consequently. Therefore, the subsequent experiments were performed at a rate of ethanol addition of 0.8 mL/min.

3.3. Loading capacity and encapsulation efficiency of SF within nanoparticles

Based on successful preparation of SF-BSA-NP with desired particle size and zeta potential, the followed drug LC and EE within nanoparticles were determined to investigate the effects of formulary and technological factors.

As shown in Fig. 3A, an improved LC of 27% was obtained with the incipient accreted ratio of BSA:SF to 2:1 (w/w). Afterward, the entrapped percent of SF within nanoparticles decreased remarkably. The increased amount of nanoparticles would have lowered the drug loading percent quickly again. On the other hand, the resulted high nanoparticles yield (above 90%) would be in favor of drug encapsulation. The more BSA used, the more desolvated BSA was involved in encapsulating the water-soluble drug dissolved in the internal aqueous phase. And the drug EE in the nanoencapsulation process was increased constantly to 85% (Fig. 3A). This high drug EE for SF-BSA-NP would be mainly attributed to the desolvated phase transition and desolvation technique of nanoencapsulation.

As for the matrix drug delivery system, hydrophobic interactions can affect the drug loading or release properties (Li et al., 2006; Wu et al., 2005). The hydrophobic tendency of protein particles induced by glutaraldehyde might also hinder the constantly encapsulation of the hydrophilic water-soluble drug SF. Fortunately surfactant could bridge the interface between

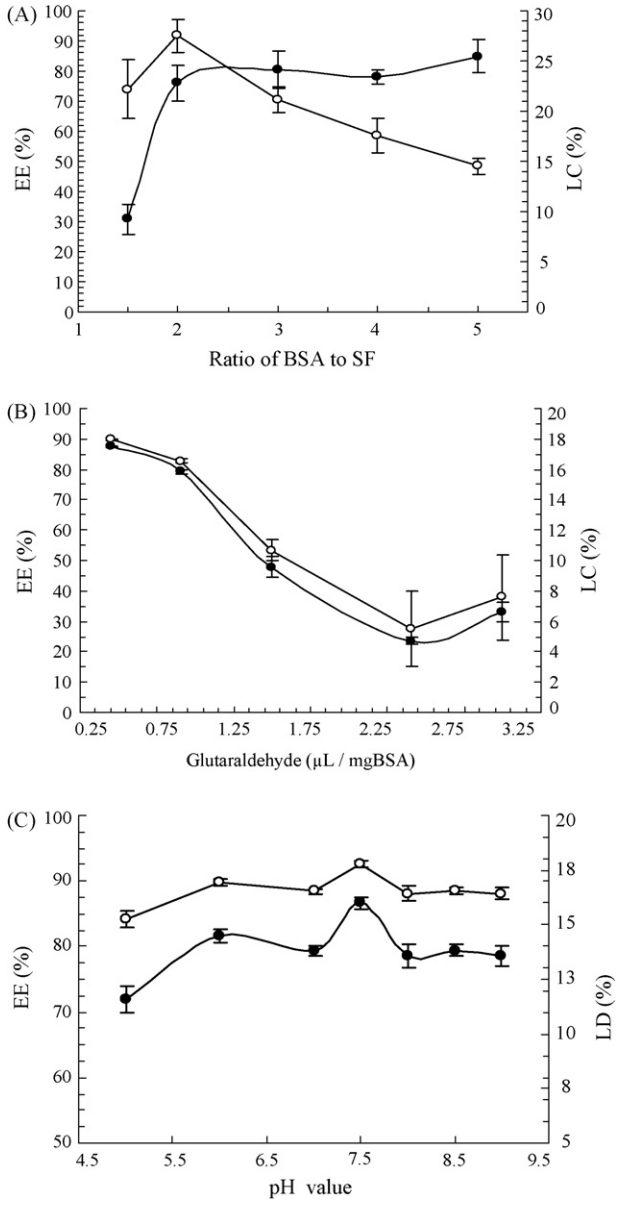

Fig. 3. Encapsulation efficiency (●) and loading capacity (◯) of SF-BSA-NP prepared with different ratios of BSA to SF (A) (ethanol addition rate 0.8 mL/min, amount of SF 12.5 mg, initial BSA concentration 6.25 mg/mL); cross-linked with different amount of 8% glutaraldehyde per mg BSA (B) (ethanol addition rate 0.8 mL/min, amount of SF 12.5 mg, rate of BSA to SF 2:1); at different pH values of the medium (C) (ethanol addition rate 0.8 mL/min, amount of SF 12.5 mg, rate of BSA to SF 2:1, cross-linked with 1.0 mL 8% glutareldehyde per mg of BSA) (mean ± S.D., $n = 3$).

the cross-linked hydrophobic carrier and the hydrophilic water-soluble drug. The addition of surfactant would balance the hydrophobic effect caused by the cross-linking agent glutaraldehyde. Considered the efficient encapsulation of the freely water-soluble drug SF, the surfactant of 0.2% (w/v) poloxamer 188 was co-mixed into the aqueous phase to encourage the loading efficiency by creating a compatible environment within the nanoparticles (Su et al., 2005).

Along with the surfactant-associated regulation effect, SF might be commonly embedded into the BSA matrix during the desolvation procedure. When cross-linked with glutaraldehyde, the drug absorbed in particle surface might diffuse into the aqueous environment. And the EE of SF was lowered during solidification of BSA nanoparticles by glutaraldehyde. It seems to be relevant to the additional decrease in hydrophilic behavior of BSA induced by the enhanced cross-linkage. Then the inlayed SF could release out from the further stabilized nanoparticles. Consequently, the drug LC and EE were dramatically decreased with the increased amounts of the cross-linker glutaraldehyde used (Fig. 3B). Along with the addition of 8% glutaraldehyde solution, the LC and EE decreased unwantedly from17.9% and 87.5% (0.45 μL/mgBSA) to 2.5% and 23.9% (2.4 μL/mgBSA), respectively. As shown from Fig. 3B, the high EE for the water-soluble SF within BSA nanoparticles decreased to about 80% after introducing 1.0 μL 8% glutaraldehyde per mg BSA. So the cross-linking agent of glutaraldehyde should be cautiously added for preparation of SF-BSA-NP. And the controlled content of glutaraldehyde would be optimized for both required drug loading and release characteristics of SF loaded BSA nanoparticles.

BSA (isoelectric point of 4.4) is a protein with amino-group and acid-group, and then the drug EE of BSA nanoparticles cross-linked with glutaraldehyde might be affected by the pH value of the medium. Considered the largely varied solubility and stability of SF in acid environment, the pH values investigated were controlled above 5.0 in the present paper.

Protein was relatively stable in the medium with pH around its isoelectric point. As for the decreased nanoparticle yield percent (under 80%) at pH 5.0, the amount of SF encapsulated into the desolvated albumin nanoparticles dropped out largely. As shown in Fig. 3C, EE (72%) and LC (15%) of SF at pH 5.0 were increased continually to 86% and 17% at pH 7.5. At the further increased pH values (Fig. 3C), drug LC or EE decreased and then kept unchanged remarkably. The decreased EE might be concerned with the accelerated cross-linking step in alkaline condition (Schiff base formed) (Lin et al., 1994). So during the desolvation procedure, the nanoencapsulation of SF should be carried out under the neutral condition.

3.4. In vitro release

The *in vitro* release profiles of SF from nanoparticles were obtained by representing the release percentage of SF with respect to the amount of SF encapsulated. For the same batch of nanoparticles, the amount of drug released *in vitro* compared well with the calculated drug LC. Fig. 4 displayed the drug release behavior of SF-BSA-NP and the effect of the cross-linker amount on release rate.

The cross-linking of BSA nanoparticles with glutaraldehyde is important for sustained release and liver-targeted drug delivery. It could be seen from Fig. 4, drug released quickly from the BSA nanoparticles not cross-linked, and the cumulative release percent exceeded 75% within 2 h. The further addition of glutaraldehyde could retard the release rate as the decreased water-solubility of BSA. In 2 h, 67% drug released from SF-BSA-NP cross-linked with 0.6 μL 8% glutaraldehyde per mg BSA. Then the drug released even more slowly with the increased amount of glutaraldehyde used, and 1.0 μL 8% glutaraldehyde per mg

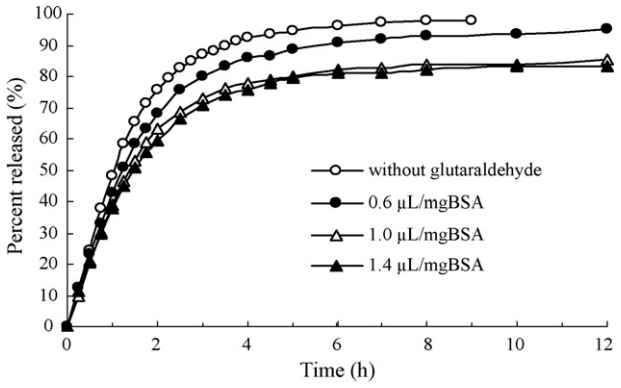

Fig. 4. *In vitro* drug release profiles of not cross-linked nanoparticles and SF-BSA-NP cross-linked with different amount of 8% glutaraldehyde in PBS (pH 7.4). Ethanol addition rate 0.8 mL/min, amount of SF 12.5 mg, rate of BSA to SF 2:1 ($n = 3$).

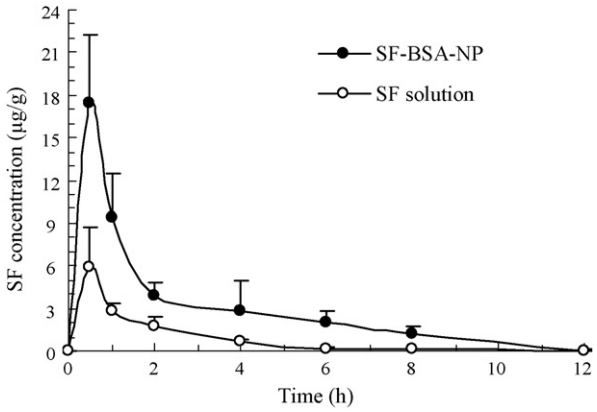

Fig. 5. Time courses of SF concentration (μg/g) in the liver of mice intravenously injected with SF-BSA-NP and SF solution (mean ± S.D., $n = 3$).

BSA might be suitable for cross-linking. The sustained-released effect could not be enhanced significantly even cross-linked with 1.4 μL 8% glutaraldehyde per mg BSA (Fig. 4). This might be explained by the limited surface free amino-groups on BSA nanoparticles and the freely water-soluble property of SF. The further augmented cross-linkage of albumin matrix seems not significantly affect the release of SF from BSA nanoparticles stabilized with 1.0 μL 8% glutaraldehyde per mg BSA. Considered the biodegradability and internalization processes of SF-BSA-NP *in vivo*, low amount of glutaraldehyde and short term should be employed in the cross-linking stage as far as possible.

It was apparent that drug release *in vitro* showed a rapid initial burst effect, and then followed by a relatively slow release rate. As shown from Fig. 4, about 20% of drug was quickly released from SF-BSA-NP within the first 0.5 h. This initial burst release was caused by the drug dispersed close to the particles surface. This part of absorbed drug could be easily desorbed from the outer layer and diffused out (Li et al., 2006). Additionally, relatively high drug loading within nanoparticles might also contribute to the burst effect. Three hours later, release profile presented a sustained release period (Fig. 4). About 85% of the entrapped drug was released from SF-BSA-NP (cross-linked with 1.0 μL 8% glutaraldehyde per mg BSA) in 12 h, which might be resulted from the diffusion out of SF embedded into the interior of the BSA matrix. The remanent material and sustained transfer could not retard the nearly complete drug-release after 12 h. The erosion and degradation of albumin might be also involved in the drug-release process.

3.5. *In vivo* biodistribution of SF-BSA-NP

Nanoparticles represent one of the promising carriers for improving the therapeutic index of the associated drugs, by increasing their localization to specific target tissues or cells and by decreasing their distribution to normal tissues (Kawashima, 2001). The concentration–time courses of SF in the mouse liver after intravenous injection were shown in Fig. 5. In almost all time periods, SF-BSA-NP showed highly hepatic drug levels compared with SF solution. It could be seen that drug concentrations for the SF-BSA-NP dosed group were two to four times than those injected with SF solution during the first 4 h. And the SF concentration in liver at 6 h for SF-BSA-NP group was nearly 10-fold that observed for SF solution group (Fig. 5). This changed drug biodistribution might have been caused by the nanoencapsulation process. And the highly hepatic distribution directly indicated the liver targeting characteristic of the prepared SF-BSA-NP. As for so much of the injected nanoparticles were distributed to the mouse liver, a murine reticuloendothelial system (RES; Kupffer cells) might be involved (Grislain et al., 1983; Yamashita et al., 1991). And the possible phagocytosis mechanism of passive targeting might be due to the high liver distribution of SF-BSA-NP.

The drug content percents in the tissues after intravenous injection were calculated by the determined SF concentrations

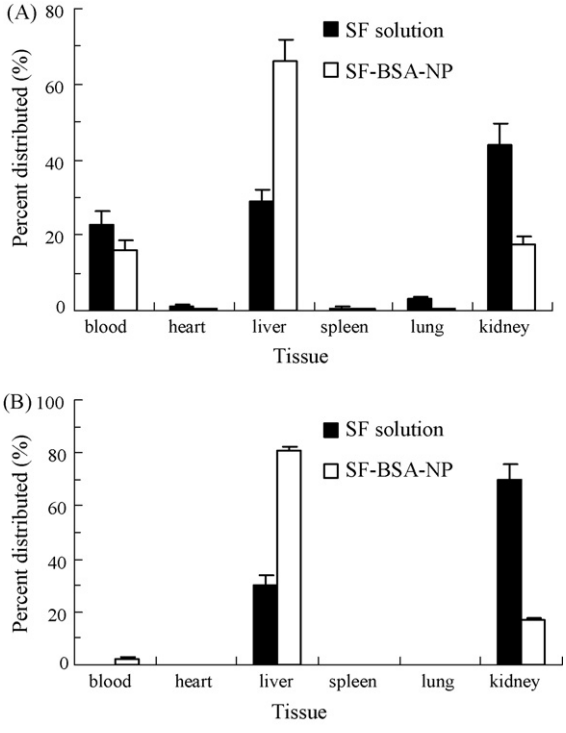

Fig. 6. Tissue distribution of SF at 1 h (A) and 12 h (B) in mice intravenously administered with SF-BSA-NP and SF solution (mean ± S.D., $n = 3$).

and organ weights. Fig. 6 shows the drug percents distributed to tissues of mice after intravenous administration with SF solution and SF-BSA-NP for 1 and 12 h. As deduced from Fig. 6, SF was mainly distributed to the circulation, liver and kidney after injection. Whereas the drug contents in heart, spleen and lung were very low. For SF-BSA-NP, the drug percents distributed to liver (66.28% for 1 h, 80.91% for 12 h) were about 2.5 times than those for SF solution (28.81% for 1 h, 30.43% for 12 h). This also suggested the hepatic tropism of the nanoencapsulated SF. In addition, the fact that considerable amount of drug appeared in kidney (Fig. 6), illustrated the mainly excretion pathway for intravenously injected SF.

Owing to the possible liver-targeted delivery route of SF-BSA-NP, much amount of SF would be efficiently accumulated and retained in the liver as compared to SF solution. And the observation correlated with those results previously reported by other authors (Mbela et al., 1992; Zhang et al., 1996; Liang et al., 2006). These data demonstrated that with the aid of nanoparticles, the anti-hepatic fibrosis agents could be importantly delivered to the liver with certain specificity whereas a subsequent reduced distribution in other organs.

4. Conclusion

The present study showed that the freely water-soluble drug SF could be encapsulated within BSA nanoparticles by a desolvation technique. The diameter and zeta potential, drug loading capacity and encapsulation efficiency of SF-BSA-NP could be modulated by adjustment of the crucial process parameters, such as, ratio of BSA to SF, concentration of glutaraldehyde and rate of ethanol addition. *In vitro* drug release profile of SF-BSA-NP showed an initial burst effect and then sustained release phase. Primary distribution test *in vivo* indicated that the negative SF-BSA-NP ranged between 100 and 200 nm could serve as a rational liver-targeted drug delivery system for future applications.

Acknowledgements

This work was supported by the National Natural Science Foundation of China (Project 30371701) and Shanghai Nanotechnology Promotion Center (Project 0452nm083).

References

Castelluccio, C., Bolwell, G.P., Gerrish, C., Rice-Evans, C., 1996. Differential distribution of ferulic acid to the major plasma constituents in relation to its potential as an antioxidant. Biochem. J. 316, 691–694.

Daemen, T., Hoedemakers, R., Storm, G., Scherphof, G.L., 1995. Opportunities in targeted drug delivery to Kupffer cells: delivery of immunomodulators to Kupffer cells-activation of tumoricidal properties. Adv. Drug Deliv. Rev. 17, 21–30.

Grislain, L., Couvreur, P., Lenaerts, V., Roland, M., Deprez-Decampeneere, D., Speiser, P., 1983. Pharmacokinetics and distribution of a biodegradable drug-carrier. Int. J. Pharm. 15, 335–345.

Harashima, H., Sakata, K., Funato, K., Kiwada, H., 1994. Enhanced hepatic uptake of liposomes through complement activation depending on the size of liposomes. Pharm. Res. 11, 402–406.

Ishida, T., Masuda, K., Ichikawa, T., Ichihara, M., Irimura, K., Kiwada, H., 2003. Accelerated clearance of a second injection of PEGylated liposomes in mice. Int. J. Pharm. 255, 167–174.

Kamruzzaman Selim, K.M., Ha, Y.S., Kim, S.J., Chang, Y., Kim, T.J., Ho Lee, G., Kang, I.K., 2007. Surface modification of magnetite nanoparticles using lactobionic acid and their interaction with hepatocytes. Biomaterials 28, 710–716.

Kawashima, Y., 2001. Nanoparticulate systems for improved drug delivery. Adv. Drug Deliv. Rev. 47, 1–2.

Klibanov, A.L., Maruyama, K., Torchilin, V.P., Huang, L., 1990. Amphipathic polyethyleneglycols effectively prolong the circulation time of liposomes. FEBS Lett. 268, 235–237.

Konno, H., Maruo, Y., Matsuda, I., Tanaka, T., Baba, S., 1997. Application of liposomes to the treatment of liver metastasis. Adv. Drug Deliv. Rev. 24, 331–335.

Langer, K., Balthasar, S., Vogel, V., Dinauer, N., von Briesen, H., Schubert, D., 2003. Optimization of the preparation process for human serum albumin (HSA) nanoparticles. Int. J. Pharm. 257, 169–180.

Li, F.Q., Hu, J.H., 2002. Advances in researches of hepatic targeted drug delivery system. Chin. Pharm. J. 37, 321–325.

Li, F.Q., Hu, J.H., Deng, J.X., Su, H., Xu, S., Liu, J.Y., 2006. In vitro controlled release of sodium ferulate from Compritol 888 ATO based matrix tablets. Int. J. Pharm. 324, 152–157.

Li, F.Q., Hu, J.H., Lu, B., Yao, H., Zhang, W.G., 2001. Ciprofloxacin-loaded bovine serum albumin microspheres: preparation and drug-release in vitro. J. Microencapsul. 18, 825–829.

Li, F.Q., Xu, S., Su, H., Deng, J.X., Liu, J.Y., Hu, J.H., 2007. Development of a gradient reversed-phase HPLC method for the determination of sodium ferulate in beagle dog plasma. J. Chromatogr. B 846, 319–322.

Liang, H.F., Chen, C.T., Chen, S.C., Kulkarni, A.R., Chiu, Y.L., Chen, M.C., Sung, H.W., 2006. Paclitaxel-loaded poly(γ-glutamic acid)-poly(lactide) nanoparticles as a targeted drug delivery system for the treatment of liver cancer. Biomaterials 27, 2051–2059.

Lin, W., Coombes, A.G.A., Davies, M.C., Davis, S.S., Illum, L., 1993. Preparation of sub-100 nm human serum albumin nanospheres using a pH-coacervation method. J. Drug Target 1, 237–243.

Lin, W., Coombes, A.G.A., Garnett, M.C., Davies, M.C., Schacht, E., Davis, S.S., Illum, L., 1994. Preparation of sterically stabilized human serum albumin nanospheres using a novel Dextranox-MPEG crosslinking agent. Pharm. Res. 11, 1588–1592.

Liu, T., Hu, J.H., Cai, Z., Shi, J., 2000. Effect of sodium ferulate on proliferation and collagen synthesis of HSC-T6 in vitro. Acad. J. Sec. Mil. Med. Univ. 21, 423–425.

Marty, J.J., Oppenheimer, R.C., Speiser, P., 1978. Nanoparticles—a new colloidal drug delivery system. Pharm. Acta Helv. 53, 17–23.

Mbela, T.K.M., Poupaert, J.H., Dumont, P., 1992. Poly(diethylmethylidene malonate) nanoparticles as primaquine delivery system to liver. Int. J. Pharm. 79, 29–38.

Merodio, M., Arnedo, A., Renedo, M.J., Irache, J.M., 2001. Ganciclovir-loaded albumin nanoparticles: characterization and in vitro release properties. Eur. J. Pharm. Sci. 12, 251–259.

Meziani, M.J., Sun, Y.P., 2003. Protein-conjugated nanoparticles from rapid expansion of supercritical fluid solution into aqueous solution. J. Am. Chem. Soc. 125, 8015–8018.

Moghimi, S.M., Hunter, A.C., Murray, J.C., 2001. Long-circulating and target-specific nanoparticles: theory to practice. Pharmacol. Rev. 58, 283–318.

Müller, G.M., Leuenberger, H., Kissel, T., 1996. Albumin nanospheres as carriers for passive drug targeting: an optimized manufacturing technique. Pharm. Res. 13, 32–37.

Nakada, Y., Fattal, E., Foulquier, M., Couvreur, P., 1996. Pharmacokinetics and biodistribution of oligonucleotide adsorbed onto poly(isobutylcyanoacrylate) nanoparticles after intravenous administration in mice. Pharm. Res. 13, 38–43.

Ogawara, K., Furumoto, K., Nagayama, S., Minato, K., Higaki, K., Kai, T., Kimura, T., 2004. Pre-coating with serum albumin reduces receptor-mediated hepatic disposition of polystyrene nanosphere: implications for rational design of nanoparticles. J. Control. Release 100, 451–455.

Rubino, O.P., Kowalsky, R., Swarbrick, J., 1993. Albumin microspheres as a drug delivery system: relation among turbidity ratio, degree of cross-linking, and drug release. Pharm. Res. 10, 1059–1065.

Smith, P.K., Krohn, R.I., Hermanson, G.T., Mallia, A.K., Gartner, F.H., Provenzano, M.D., Fujimoto, E.K., Goeke, N.M., Olson, B.J., Klenk, D.C., 1985. Measurement of protein using bicinchoninic acid. Anal. Biochem. 150, 76–85.

Song, C.X., Labhasetwar, V., Murphy, H., Qu, X., Humphrey, W.R., Shebuski, R.J., Levy, R.J., 1997. Formulation and characterization of biodegradable nanoparticles for intravascular local drug delivery. J. Control. Release 43, 197–212.

Souto, E.B., Anselmi, C., Centini, M., Müller, R.H., 2005. Preparation and characterization of n-dodecyl-ferulate-loaded solid lipid nanoparticles (SLN®). Int. J. Pharm. 295, 261–268.

Su, H., Hu, J.H., Li, F.Q., 2005. Effects of surfactants on the pharmaceutical characteristics of bovine serum albumin nanoparticles of highly water-soluble drug sodium ferulate. Pharm. Care Res. 5, 153–156.

Tröster, S.D., Müller, U., Kreuter, J., 1990. Modification of the body distribution of poly(methyl methacrylate) nanoparticles in rats by coating with surfactants. Int. J. Pharm. 61, 85–100.

Wang, B.H., Ou-Yang, J.P., 2005. Pharmacological actions of sodium ferulate in cardiovascular system. Cardiovasc. Drug Rev. 23, 161–172.

Wang, H., Peng, R.X., Wang, R.K., Kong, R., 1997. Antagonizing effect of sodium ferulate on the changes of hepatic antioxidative function induced by ethanol in mice. Acta Pharm. Sin. 32, 511–514.

Weber, C., Coester, C., Kreuter, J., Langer, K., 2000. Desolvation process and surface characteristics of protein nanoparticles. Int. J. Pharm. 194, 91–102.

Williams, J., Lansdown, R., Sweitzer, R., Romanowski, M., LaBell, R., Ramaswami, R., Unger, E., 2003. Nanoparticle drug delivery system for intravenous delivery of topoisomerase inhibitors. J. Control. Release 91, 167–172.

Wu, J., Danielsson, A., 1994. Inhibition of hepatic fibrogenesis: a review of pharmacologic candidates. Scand. J. Gastroenterol. 29, 385–391.

Wu, Z., Joo, H., Lee, T.G., Lee, K., 2005. Controlled release of lidocaine hydrochloride from the surfactant-doped hybrid xerogels. J. Control. Release 104, 497–505.

Yamashita, C., Matsuo, H., Akiyama, K., Kiwada, H., 1991. Enhancing effect of cetylmannoside on targeting of liposomes to Kupffer cells in rats. Int. J. Pharm. 70, 225–233.

Yao, T., Huang, L., Zern, M.A., 1995. The use of liposomes in the therapy of liver disease. Adv. Drug Deliv. Rev. 17, 239–246.

Zhang, Z.R., Liao, G.T., Nagai, T., Hou, S.X., 1996. Mitoxantrone polybutyl cyanoacrylate nanoparticles as an anti-neoplastic targeting drug delivery system. Int. J. Pharm. 139, 1–8.

Zimmer, A.K., Maincent, P., Thovenot, P., Kreuter, J., 1994a. Hydrocortisone delivery to healthy and inflamed eyes using a micellar polysorbate 80 solution or albumin nanoparticles. Int. J. Pharm. 110, 211–222.

Zimmer, A.K., Zerbe, H., Kreuter, J., 1994b. Evaluation of pilocarpine-loaded albumin particles as drug delivery systems for controlled delivery in the eye. I. In vitro and in vivo characteristics. J. Control. Release 32, 57–70.